Indian Journal of Chemistry
Vol. 64, March 2025, pp. 306-315
DOI: 10.56042/ijc.v64i3.16605

# Development of a gelatin-halloysite nanotube-carrageenan polyelectrolyte complex for *p*H-responsive oral delivery of lipoic acid

Dikshita Sharma & Tarun K Maji*

Department of Chemical Sciences, Tezpur University, Napaam, Sonitpur 784 028, Assam, India

E-mail: tkm@tezu.ernet.in

*Receivaed 28 January 2025; accepted (revised) 27 February 2025*

This study investigates the formulation and characterisation of a novel glutaraldehyde crosslinked gelatin-halloysite nanotube-carrageenan (GHC) polyelectrolyte complex (PEC) designed for the controlled oral delivery of lipoic acid, a therapeutic agent limited by poor solubility and instability in acidic environments. The properties of the complex were studied with respect to the variation of concentration of crosslinker and nanofiller. The *p*H-responsive release mechanism of the composite was evaluated under simulated gastrointestinal conditions, showing minimal drug release in acidic conditions and substantially increased release at intestinal *p*H levels. Characterisation through Fourier Transform Infrared Spectroscopy (FTIR) and X-ray Diffraction (XRD) confirmed the structural integrity and successful drug encapsulation within an amorphous matrix. Biological assays, including glucose uptake and cell viability studies, validated the composite's bioactivity and non-toxic nature, emphasising its potential for enhancing lipoic acid's bioavailability and therapeutic efficacy. The findings demonstrate the GHC complex's capability to provide a targeted, controlled release, positioning it as a promising system for advanced drug delivery applications.

**Keywords**: Biopolymer, Controlled drug delivery, Diabetes, Sustained hypoglycaemia, Targeted drug delivery

Lipoic acid, a potent antioxidant with therapeutic applications in diabetes, neurodegenerative disorders, and cardiovascular diseases, faces significant challenges in oral administration due to its poor water solubility and instability in acidic environments[1,2]. It undergoes rapid degradation upon exposure to gastric conditions, leading to reduced bioavailability and therapeutic efficacy[3]. To address these limitations, pharmaceutical research has focused on developing advanced drug delivery systems that offer sustained release and *p*H-responsive behaviour[4,5].

Biopolymer-based delivery systems have gained considerable attention owing to their biocompatibility, biodegradability, and tunable physicochemical properties[6]. Gelatin, a natural polymer derived from collagen, is extensively used in drug delivery applications due to its excellent film-forming ability, biocompatibility, and enzymatic degradability[7,8]. However, gelatin alone may lack the mechanical strength and stability required for effective gastrointestinal transit[9]. Composite systems incorporating nanomaterials and additional biopolymers have been explored to enhance its performance[10].

Halloysite nanotubes (HNTs), naturally occurring aluminosilicate clays with a unique hollow tubular structure, have emerged as promising nanocarriers for drug delivery[11]. The high surface area, biocompatibility, and ability to load hydrophilic and hydrophobic drugs make HNTs ideal for sustained-release applications. The dual surface chemistry of HNTs—with silica-rich outer and alumina-rich inner surfaces—facilitates the adsorption and encapsulation of drug molecules like lipoic acid[12]. Additionally, carrageenan, a sulfated polysaccharide extracted from red seaweeds, exhibits *p*H-responsive gelation behaviour, making it suitable for targeted drug delivery to the intestinal tract[13]. Carrageenan's ability to remain stable in acidic gastric conditions and to swell and degrade in the neutral to alkaline *p*H of the intestine enhances site-specific drug release characteristics[14].

In this study, we have developed a novel gelatin–halloysite nanotube–carrageenan composite system for the oral delivery of lipoic acid. The system leverages the synergistic properties of its components to achieve sustained release and *p*H-responsive behaviour. The incorporation of HNTs enhances the encapsulation efficiency. It provides a sustained release matrix, while carrageenan imparts *p*H sensitivity, promoting minimal drug release in the acidic stomach environment and enhanced release at intestinal *p*H. This approach aims to improve lipoic

acid's bioavailability and therapeutic efficacy by protecting it from premature degradation and enabling targeted delivery to the absorption site.

## Experimental Section

Carrageenan Type I, consisting primarily of λ and a smaller proportion of κ-carrageenan, was acquired from Sigma-Aldrich Inc. (USA). Gelatin type A was also sourced from Sigma-Aldrich Inc. (USA). Glacial acetic acid (E. Merck, India), Tween 80 (E. Merck, India), and double-distilled deionised (DDI) water were utilised consistently throughout the study. All other chemicals used were of analytical grade.

### Preparation of glutaraldehyde crosslinked lipoic acid loaded gelatin-haloysite-carrageenan polyelectrolyte complex (PEC)

The gelatin-carrageenan complex was created using a previously described method, with minor adjustments made[12–14]. 100 mL of a 0.3% (w/v) carrageenan solution was prepared in water and placed into a beaker. It was stirred vigorously using a stirrer under high agitation at 70°C. A known amount of HNT (0-0.06g) pre-dispersed in water by constant stirring for 24h followed by sonication, was added to the carrageenan under continuous stirring. Tween 80 was added to the mixture to ensure uniform dispersion. Separately, α-lipoic acid (0.01g) dissolved in a 1:1 ethanol-water solution was added very slowly to the carrageenan-HNT solution, and constant stirring was maintained for 2-3 h. A known amount of (200 mL) gelatin A solution of 1% (w/v) was added to the beaker dropwise to attain complete phase separation. However, the weight ratio of carrageenan to gelatin was maintained at 1:2 during all the experiments. The interaction between gelatin and carrageenan occurred completely at this ratio per the coacervate % yield and viscosity measurements.[12] The *p*H of the mixture was then brought down to 3.5 by adding 2.5% (v/v) glacial acetic acid solution. The temperature was then lowered to 0-5°C. At this point, glutaraldehyde (0-15μL) was added dropwise to the mixture, and the temperature was raised to 45°C. Stirring was maintained for 3-4 h to facilitate cross-linking. The resulting suspension was allowed to cool to RT and centrifuged. The product thus obtained was freeze-dried. In this way, a series of samples were prepared by varying the concentrations of crosslinker and halloysite as shown in Table 1.

### Calculation of process yield

The process yield was determined using the following equation[15].

$$\text{Process yield}(\%) = \frac{\text{Weight of the product}}{\text{Weight of(Drug+HNT+Polymer)}} \times 100 \quad \ldots (1)$$

### Calibration curve of lipoic acid

A calibration curve is essential for determining the drug's loading, encapsulation efficiency, and release rate from the complex within an appropriate solvent medium (ethanol-water), and it is plotted following the established protocol[16].

A series of known concentrations of α-Lipoic acid (prepared in double-distilled water) were analysed using a UV-Vis spectrophotometer (UV-2001, Hitachi, Tokyo, Japan) across the 200–600 nm wavelength range. A characteristic absorbance peak was observed between 227 and 334 nm, corresponding to α-Lipoic acid concentrations ranging from 0.001 to 0.005 g per 100 mL (Fig. 1).

Table 1 — Effect of GA and HNT on properties of Lipoic Acid loaded Gelatin-Carrageenan complex*

| Sample Code[(a)] | Gelatin % w/v (amount in g in 50 mL water) | Carrageenan % w/v (amount in g in 50 mL water) | Amount of crosslinker, % v/w (in μL) | Amount of HNT clay, % w/w w.r.t. GC (g in 50mL water) | Process Yield (%) | Encapsulation Efficiency (%) | Drug Loading Efficiency (%) |
|---|---|---|---|---|---|---|---|
| GC | 0.1 (0.05) | 0.3 (0.15) | 0 | 0 | 72.3 (±0.02) | 80.3 (±0.02) | 53.2 (±0.03) |
| GC/GA1 | 0.1 (0.05) | 0.3 (0.15) | 2.5 (5) | 0 | 71.5 (±0.03) | 79.5 (±0.04) | 51.8 (±0.04) |
| GC/GA2 | 0.1 (0.05) | 0.3 (0.15) | 5.0 (10) | 0 | 77.1 (±0.02) | 76.8 (±0.02) | 49.3 (±0.02) |
| GC/GA3 | 0.1 (0.05) | 0.3 (0.15) | 7.5 (15) | 0 | 69.8 (±0.01) | 75.1 (±0.05) | 41.9 (±0.05) |
| GC/H1 | 0.1 (0.05) | 0.3 (0.15) | 0 | 0.3 (0.06) | 80.8 (±0.03) | 80.8 (±0.04) | 56.4 (±0.04) |
| GC/H2 | 0.1 (0.05) | 0.3 (0.15) | 0 | 1.2 (0.24) | 79.5 (±0.04) | 81.2 (±0.05) | 58.2 (±0.01) |
| GC/H3 | 0.1 (0.05) | 0.3 (0.15) | 0 | 4.8 (0.96) | 82.1 (±0.01) | 83.4 (±0.01) | 59.9 (±0.04) |
| GC/GA2/H2 | 0.1 (0.05) | 0.3 (0.15) | 5.0 (10) | 1.2 (0.24) | 80.63 (±0.04) | 79.2 (±0.03) | 55.3 (±0.01) |

Lipoic Acid = 0.01g, Tween 80 = 0.015 mL.

In the sample code, Gelatin-Carrageenan PEC, glutaraldehyde, and HNT are represented by "GC," "GA," and "H," respectively.

* Each value and the standard deviation in parentheses represent the average of five readings.

The absorbance values at 227–334 nm for each concentration were recorded and plotted, generating a calibration curve showing a linear relationship between absorbance and concentration. This calibration curve was subsequently used to estimate the unknown concentrations of α-Lipoic acid in release studies based on the measured absorbance values at the corresponding wavelength.

### Calculation of encapsulation efficiency and drug loading efficiency of the polyelectrolyte complex

After ultracentrifuging the samples at RT for 30 minutes, the drug loading efficiency (LE) and encapsulation efficiency (EE) from different formulations were assessed. The concentration of unencapsulated α-Lipoic acid in the supernatant was determined by measuring its absorbance at wavelengths between 227 and 334 nm using a UV-Vis spectrophotometer. The encapsulation efficiency (EE) was then calculated using a standard formula, as outlined in the relevant literature[17].

$$Loading\ efficiency(LE)\% = \frac{(Total\ amount\ of Drug - Free\ amount\ of drug)}{Total\ amount\ of\ drug} \times 100 \quad \ldots (2)$$

$$Encapsulation\ efficiency(EE)\% = \frac{(Total\ amount\ of Drug - Free\ amount\ of\ drug)}{Weight\ of\ dry\ polyectrolyte\ complex} \times \quad \ldots (3)$$

### *In vitro* drug release studies

Dried samples containing α-Lipoic acid (LA)-loaded complexes were weighed and immersed in phosphate buffer solutions at *p*H 1.2 and 7.4 to simulate gastric and intestinal *p*H, respectively. The samples were continuously stirred in these solutions to simulate drug release under physiological conditions. At predetermined time intervals, 5 mL of the solution was withdrawn, filtered, and analysed spectrophotometrically at 227–334 nm using a UV-Vis spectrophotometer to measure the cumulative drug release at each time point. An equal amount (5 mL) of fresh buffer solution at the corresponding *p*H was added to the beaker to maintain a constant volume. This process was repeated three times for each determination to ensure reproducibility[18,19].

### Characterisation

#### Fourier transform infrared spectroscopy study

A spectrophotometer model Impact-410 by Nicholet was used to record the Fourier transform infrared (FTIR) spectra in the 4,000–400 $cm^{-1}$ range

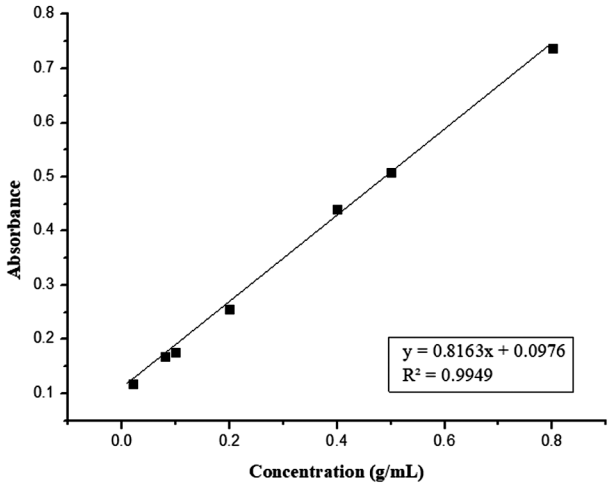


Fig. 1 — Calibration curve of Lipoic Acid

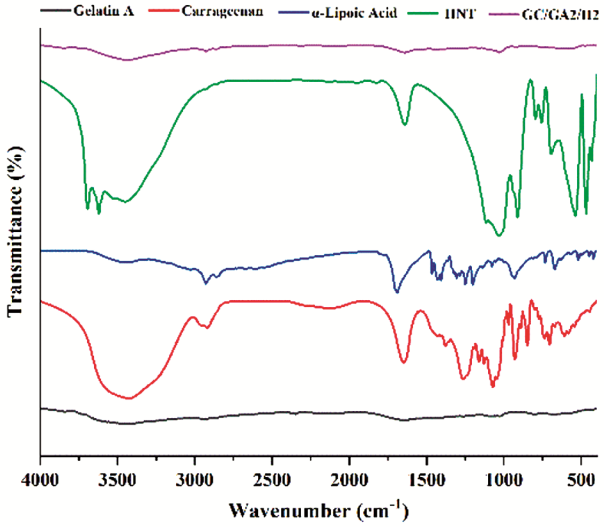


Fig. 2 — FTIR spectra of the product and the raw materials

(Fig. 2). Gelatin A, carrageenan, α-lipoic acid, HNT, and lipoic acid-loaded gelatin-HNT-carrageenan PEC were each finely grounded with KBr separately and prepared for the spectroscopy study.

### X-ray diffraction study

X-ray diffractograms of α-lipoic acid and glutaraldehyde crosslinked lipoic acid loaded gelatin-HNT-carrageenan complex were recorded on an X-ray diffractometer to determine the crystallinity distribution of Lipoic acid and the intercalation in the polymer complex (Fig. 3). A Rigaku X-ray diffractometer (Miniflax, UK) was used to scan the samples from 2Θ=10° to 80°, with a scanning rate of 1°/min, using CuKα (λ=0.15nm) radiation.

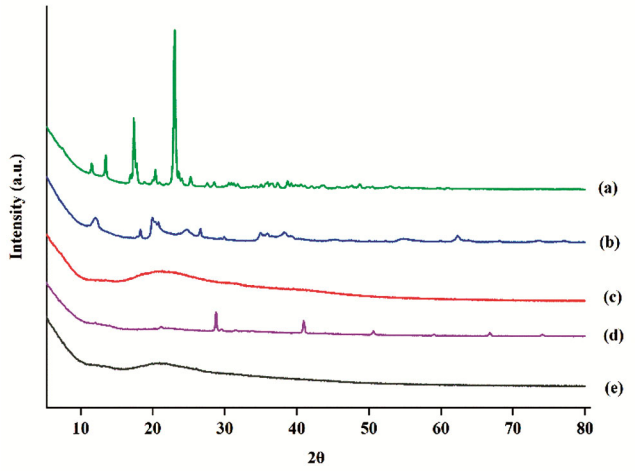


Fig. 3 — XRD Pattern of (a) Lipoic Acid, (b) Halloysite, (c) Gelatin, (d) Carrageenan and (e) GC/GA2/H2

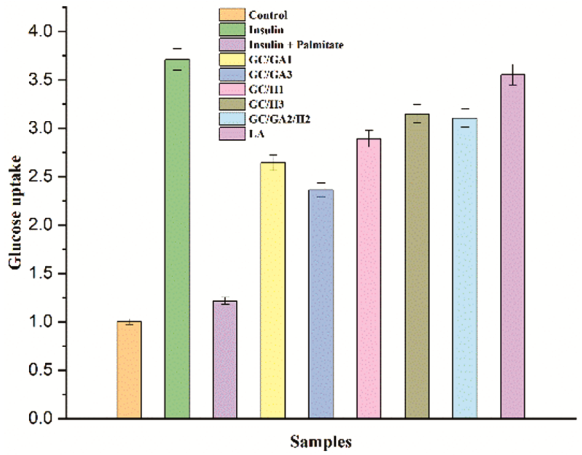


Fig. 4 — Glucose uptake assay results for the samples

## Field Emission Scanning electron microscope study

Surface morphology was studied using field emission scanning electron microscopy. The samples were studied using a field emission scanning electron microscope (GEMINI 500) with an operating voltage range of 0.2–30 kV.

## Glucose uptake assay

The glucose uptake assay (Fig. 4) used a cell-based assay kit (Cayman, USA) and followed a previously documented method[20,21]. L6 myotubes were starved of serum overnight in Kreb's Ringer Phosphate (KRP) buffer with 0.2% bovine serum albumin (BSA). The cells were then treated with LA-loaded gelatin-carrageenan PEC having varied concentrations of crosslinker (GA) and HNT for 1 h, followed by palmitate (0.75 mM) incubation for 6 h and 30 min. Insulin (100 nM) was administered before concluding the incubations. 2-NBDG, a fluorescently labelled glucose analogue, was added 5 min before ending the experiment in each incubator. Subsequently, the cells were lysed, and the fluorescent intensity was measured using the Varioskan LUX Multimode Microplate Reader (Thermo Scientific, Finland). Each sample was tested in triplicate.

## Cell viability assay

Cell viability was determined using the MTT assay, following a previously described protocol[22,23]. Differentiated THP-1 macrophages were seeded in 96-well plates and exposed to various concentrations of the drug formulation for 24 h. After treatment, 10 µL of MTT reagent (5 mg/mL in PBS) was added to each well and incubated for 4 h at 37°C. The resulting formazan crystals were dissolved in 100 µL of acidic isopropanol and further incubated for 30 min at 37°C. Cytotoxicity was assessed by measuring absorbance for each sample in three different concentrations (20µg/µL, 40µg/µL, 100µg/µL) at 570 nm using a Multiskan GO Microplate Spectrophotometer (Thermo Scientific, Finland). Absorbance values were blanked against wells containing only acidic isopropanol, and untreated cells (exposed to medium only) were used as the control, representing 100% cell viability. Each assessment was performed in triplicate.

## Statistical analysis

The data underwent statistical analysis using one-way analysis of variance (ANOVA), with $p < 0.05$ considered statistically significant and expressed as means ± standard deviation (SD). Error bars in graphs indicate the standard deviation from three independent experiments.

## Results and Discussion

### Process yields, drug encapsulation efficiency, and drug loading efficiency

The process yield was calculated using the formula provided in Equation (1), and Table 1 presents the yield, encapsulation efficiency, and drug loading efficiency results for various Gelatin A/Carrageenan-based polymer systems developed for delivering lipoic acid (LA). These results highlight the effects of varying halloysite nanotube (HNT) and glutaraldehyde (GA) concentrations on the properties of the complexes.

HNT and GA concentration variations do not exhibit any specific trend in process yield (%). The irregular trend is possibly due to material loss during isolation, a phenomenon also observed in other crosslinked polymeric systems. When examining encapsulation and loading efficiencies, a notable trend emerged: as the HNT content increased, both encapsulation efficiency and drug loading efficiency improved. This enhancement can be attributed to the nanotubular structure and high aspect ratio of HNT, which provide additional surface area and facilitate more robust intermolecular interactions between the drug and the polymeric matrix[24]. Specifically, the abundant –OH groups on the HNT surface can form hydrogen bonds with functional groups of Gelatin A ($–NH_2$, –COOH) and carrageenan ($–SO_4$, –COOH), encouraging the polymer chains to adopt extended or more rigid conformations[25]. These structural modifications create a more organised and compact matrix environment that can better retain the drug molecules, thus boosting encapsulation and loading efficiencies.

The interaction of HNT with the polymer network can also lead to the forming of a porous structure during dehydration, which includes small channels extending from the interior to the outer surface of the complex[26]. While such porosity is sometimes associated with enhanced drug release, careful optimisation of HNT content and crosslinking density can counterbalance premature diffusion, ultimately supporting higher encapsulation and loading[27]. Further, incorporating GA as a crosslinker may reduce polymer chain mobility, encouraging network rigidity and potentially increasing porosity. At elevated GA concentrations, these changes could allow the drug to migrate through pores and channels from the complex interior to the surrounding medium, thereby diminishing encapsulation and loading efficiencies[28]. However, the positive effects of HNT incorporation can mitigate these losses by providing a more structured and interactive environment for the drug.

Overall, increasing HNT concentration fosters a more favourable microenvironment for drug retention within Gelatin A/Carrageenan complexes, enhancing encapsulation and loading efficiencies, even in increased cross-linking. This improvement aligns with observations in other biopolymer-HNT composites, where nanotube inclusion improves drug loading capacity, demonstrating the versatile applicability of HNT in drug delivery systems.

### *In vitro* release studies

The *in vitro* release profile of lipoic acid (LA) from the glutaraldehyde-crosslinked gelatin-halloysite-carrageenan polyelectrolyte complex was investigated for 1 to 50 h at two *p*H levels, 1.2 and 7.4. The cumulative release percentage of LA was found to be *p*H-dependent, with higher release rates observed in the alkaline medium (*p*H 7.4) compared to the acidic medium (*p*H 1.2).

At *p*H 1.2, gelatin molecules become protonated, enhancing their electrostatic interactions with the negatively charged sulfate groups of carrageenan. This results in forming a more compact and denser polyelectrolyte complex, which reduces the matrix's swelling capacity and restricts the diffusion of LA. Consequently, the rate of LA release decreases in the acidic environment due to the tighter network structure that limits solvent penetration.

In contrast, at *p*H 7.4, deprotonation of gelatin reduces its interaction with carrageenan, leading to a looser polymer network. This increases the swelling of the complex, allowing more solvent access to the encapsulated LA. The breakdown of hydrogen bonds between the polymer matrix and LA at higher *p*H levels promotes drug release, resulting in a higher cumulative release percentage. The enhanced swelling under alkaline conditions improves the diffusion pathways for LA, thereby accelerating its release from the complex.

The data also demonstrated that the cumulative release of LA decreased with increasing concentrations of halloysite nanotubes (HNTs) and glutaraldehyde (GA). Incorporating HNTs introduces silicate layers that act as physical barriers, impeding solvent molecules from penetrating the complex. Higher HNT content intensifies this barrier effect, restricting solvent access to the encapsulated LA and thus decreasing its release rate.

Similarly, increasing the GA concentration enhances the crosslinking density within the polyelectrolyte complex. A higher degree of crosslinking results in a more rigid and less permeable network structure, further limiting solvent diffusion. This denser matrix effectively traps LA, leading to a decrease in its cumulative release over time.

These findings suggest that by modulating the *p*H and adjusting the concentrations of HNTs and GA, it is possible to control the release profile of LA from the gelatin-halloysite-carrageenan polyelectrolyte complex. The ability to tailor the drug release

behaviour makes this system a promising candidate for targeted and controlled drug delivery applications.

## Characterisation

### Fourier transform infrared spectroscopy

Gelatin-A typically displays broad absorptions for N–H and O–H stretching between 3100 and 3400 $cm^{-1}$, indicative of both peptide backbone amides and bound water. Its amide I band (~1650 $cm^{-1}$) corresponds primarily to C=O stretching of peptide bonds, while the amide II band (~1540 $cm^{-1}$) arises from N–H bending and C–N stretching[29]. Carrageenan, a sulfated polysaccharide, presents a broad O–H stretching region around 3200–3400 $cm^{-1}$, reflecting its extensive hydrogen-bonding network. Its sulfate ester groups yield characteristic S=O stretching vibrations typically observed near 1220–1250 $cm^{-1}$. The carrageenan backbone's glycosidic C–O–C stretches appear in the 1000–1150 $cm^{-1}$ range[30]. Formation of the polyelectrolyte complex through electrostatic interactions between the positively charged regions of gelatin and the negatively charged sulfate groups of carrageenan led to subtle shifts in these bands. Such shifts and changes in intensity ratios in the amide and sulfate regions confirm the establishment of intermolecular interactions within the hybrid matrix.

The use of glutaraldehyde as a crosslinker typically induces minor shifts in the amide I and II regions due to the formation of covalent bonds between the aldehyde groups and the free amino residues in gelatin. This crosslinking can slightly increase the rigidity of the biopolymer network and may lead to small wavenumber shifts or intensity changes in the amide I band[31]. The addition of halloysite nanotubes introduces characteristic signals of aluminosilicate structures. Si–O–Si and Al–O–Si stretching vibrations generally occur between 1000 and 1100 $cm^{-1}$ (Ref. 32). The presence of these absorptions in the composite's spectrum confirmed the successful incorporation of HNT. The interaction between the biopolymeric matrix and HNT surfaces broadened or slightly shifted polymeric bands, reflecting hydrogen bonding or electrostatic interactions at the organic-inorganic interface.

Encapsulated lipoic acid (LA), containing a carboxylic acid moiety, contributes disinct C=O stretching bands in the approximately 1700–1720 $cm^{-1}$ region[33]. The O–H stretch of the carboxyl group appears as a broad absorption, overlapping with the biopolymers' broad O–H/N–H region. Although the disulfide bond of LA is weakly IR-active, its presence can nonetheless influence the local chemical environment. Interactions between LA and the gelatin–carrageenan–HNT matrix led to subtle spectral changes, particularly in regions associated with hydrogen bonding and carbonyl absorptions.

The IR spectrum of GC/GA2/H2 reflects the characteristic functional groups of each component and the interactions that arise from their combination. The encapsulation of lipoic acid within this matrix introduces additional features, most notably related to the presence of its carboxylic acid groups.

The IR spectral data validate the formation of a structurally coherent, crosslinked gelatin–carrageenan polyelectrolyte complex incorporating halloysite nanotubes and encapsulating lipoic acid. Characteristic amide (gelatin), sulfate and glycosidic (carrageenan), silicate (HNT), and carboxylic (LA) absorptions are evident. Shifts in key bands, notably in the amide and sulfate regions, and the appearance of distinct carbonyl peaks from LA's carboxylic groups confirm the successful integration of each component. These spectral signatures collectively demonstrate the establishment of intermolecular interactions, improved matrix rigidity through crosslinking, and effective encapsulation of lipoic acid.

### X-ray diffraction study

Lipoic acid (LA) exhibits distinct sharp peaks at $2\theta = 23°$ and $2\theta = 19°$, which indicate its crystalline nature. The diffractogram of the GC system showed a distinct broad peak at $2\theta = 21°$. The characteristic peaks for lipoic acid disappeared in the diffractogram of the drug-loaded complex. This suggests the formation of an amorphous region, likely due to the suppression of the drug's crystallisation within the confinement of the polymer matrix[34,35]. This also indicates the molecular-level dispersion of LA within the complex and the amorphous or disordered crystalline nature of LA in the polymer matrix. The transition to an amorphous state " (as suggested by the disappearance of these peaks in Fig. 5 for drug-loaded formulations) can significantly enhance the drug's solubility and bioavailability.

### Field-Emission Scanning Electron Microscopy (FESEM) analysis

FESEM was employed to investigate the surface morphology of the Gelatin-Halloysite Nanotube (HNT)-Carrageenan polyelectrolyte complexes loaded with lipoic acid. The pristine gelatin matrix exhibited

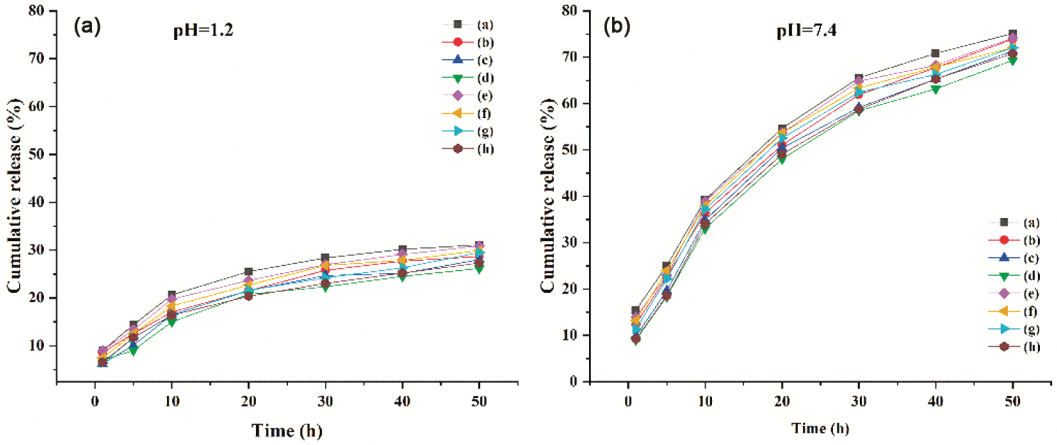


Fig. 5 — The cumulative drug release profile for (a) GC, (b) GC/M1, (c) GC/M2, (d) GC/M3, (e) GC/GA1, (f) GC/GA2, (g) GC/GA3, (h)GC/GA2/M2

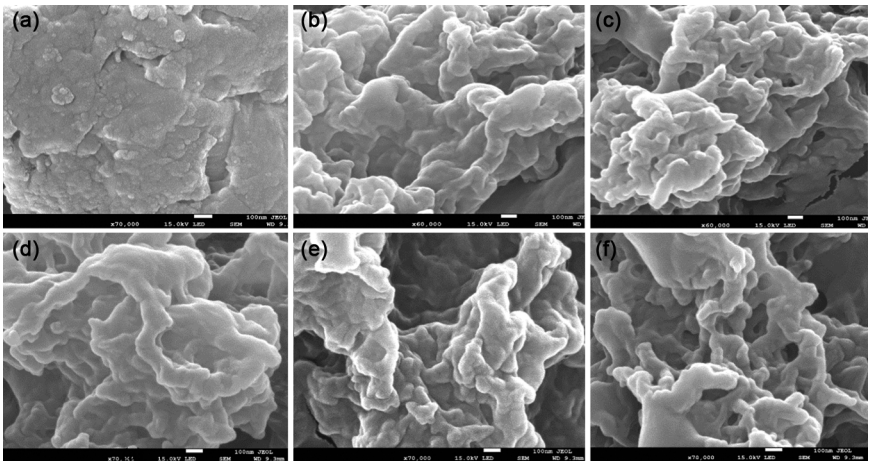


Fig. 6 — FESEM images of (a) GC, (b) GC/GA1, (c) GC/GA3, (d) GC/M1, (e) GC/M3, (f) GC/GA2/M2

a relatively smooth and continuous surface (Fig. 6a). Subtle surface irregularities emerged after incorporating HNTs at lower concentrations (Fig. 6b), suggesting initial HNT dispersion within the polyelectrolyte network. These nanotubes, which inherently possess elongated tubular structures, remained partially embedded within the gelatin-carrageenan matrix, producing mild undulations without substantial agglomeration.

As the HNT concentration increased (Fig. 6c), the surface became more textured, indicative of enhanced nanotube aggregation and stronger polymer-nanotube interactions. This texturisation has been associated with hydrogen bonding and electrostatic attractions among the negatively charged carrageenan, positively charged gelatin segments, and the aluminosilicate framework of HNT, resulting in a denser polymer network[36]. Furthermore, adding crosslinking agents at higher concentrations (Fig. 6e) led to more pronounced matrix densification, manifested by tighter structural features and increased roughness on the complex surface. These modifications suggest efficient crosslinking between the amine groups of gelatin and the sulfate groups of carrageenan, further stabilised by interactions with HNT.

Incorporating both HNT and crosslinkers thus yielded polyelectrolyte complexes with enhanced textural complexity compared to their HNT-free counterparts. Such roughened surfaces are advantageous for site-specific oral drug delivery as they can promote stronger adhesion to the intestinal mucosa, prolonging local residence time and improving therapeutic effectiveness. These nanotubes may also contribute to the *p*H-responsive release of lipoic acid, as the interpolymeric crosslinks can undergo conformational changes in varying gastrointestinal *p*H conditions, optimising drug release profiles (Fig. 5 and Fig. 4) for improved bioavailability[37].

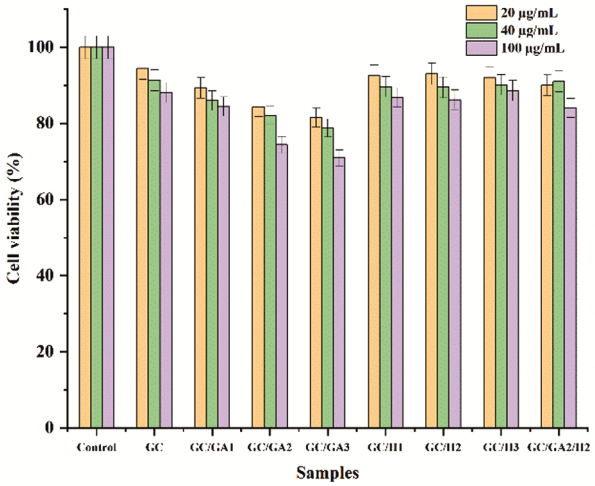


Fig. 7 — Cytotoxicity assay performed for the lipoic acid-loaded GC systems with varying concentrations of GA and HNT

## NBDG uptake assay

The 2-NBDG uptake assay was employed to evaluate the effects of lipoic acid-loaded gelatin–carrageenan nanoparticles, which were prepared by varying the concentration of glutaraldehyde (GA) crosslinking agent and Halloysite nanotubes (HNT) on glucose uptake in L6 myotubes. The assay results indicate that crosslinking density and HNT concentration significantly influence cellular metabolic activity.

As expected, untreated control cells presented baseline 2-NBDG uptake, whereas insulin-treated cells presented a marked increase in glucose uptake (Fig. 7, samples a and b). This positive control confirmed the assay's sensitivity in detecting increased glucose uptake under conditions of enhanced insulin sensitivity. In contrast, cotreatment with insulin and palmitate significantly reduced glucose uptake (Fig. 4, sample c), consistent with the literature on fatty acid-induced insulin resistance and impaired insulin signalling, thereby reducing glucose uptake in muscle cells[38,39]. This condition serves as a model of metabolic impairment, providing a comparative basis for assessing nanoparticle efficacy in potentially restoring or enhancing glucose uptake.

The lipoic acid-loaded formulations with higher GA concentrations (Fig. 4, samples d: GC/GA3 and e: GC/GA2) corresponded to a notable decrease in 2-NBDG uptake relative to insulin-treated cells. This trend aligns with previous studies indicating that increased crosslinking density can result in reduced nanoparticle flexibility and diminished cellular interaction, thereby hindering metabolic function[40]. Reduced flexibility from increased crosslinking density likely limits the nanoparticles' cellular uptake, attenuating lipoic acid's bioavailability and potential effects on glucose metabolism. In contrast, nanoparticles with a lower crosslinking density (Fig. 4, sample f: GC/GA1) maintained relatively high glucose uptake. These findings suggest moderate crosslinking levels may support structural stability without significantly compromising cellular uptake. A balanced degree of crosslinking appears to be critical for optimal interactions with cellular membranes, enhancing the metabolic effects of curcumin.

Variations in the HNT concentration within the nanoparticles also affected 2-NBDG uptake. The increase in HNT concentration in the PECs corresponded to an increase in glucose uptake, suggesting that HNT at these levels may positively influence cellular bioactivity. The combined formulation with moderate GA crosslinking and HNT (Fig. 4, sample h: GC/GA2/H2) also demonstrated good glucose uptake.

Lipoic acid alone (Fig. 4, sample l) increased glucose uptake. Curcumin modulates inflammatory pathways and antioxidant responses, alleviating cellular stress and enhancing glucose uptake. This result aligns with the hypothesis that lipoic acid can positively impact glucose metabolism even when delivered without additional modifications, highlighting its therapeutic potential in metabolic disorders[41].

Overall, the 2-NBDG uptake results suggest that lipoic acid-loaded gelatin–carrageenan nanoparticles, particularly those with lower GA crosslinking and higher HNT concentrations, enhance glucose uptake in L6 myotubes. The optimal balance of GA and HNT is essential to maintain biocompatibility and maximise glucose uptake.

## Cell viability assay

Cell viability was evaluated using an MTT assay in differentiated THP-1 macrophages exposed to various concentrations (20 µg/µL, 40 µg/µL, 100 µg/µL) of lipoic acid-loaded gelatin-carrageenan polyelectrolyte complexes (PECs), which were modified by differing concentrations of glutaraldehyde (GA) and halloysite nanotubes (HNT). Untreated cells were employed as controls, establishing a baseline viability of 100%, which is essential for assessing the relative impact of each formulation.

Cells treated with the base gelatin-carrageenan formulation (GC) exhibited near-baseline viability at 20 μg/μL (Fig. 7). However, increasing the concentration resulted in a modest decrease in viability, suggesting that the polymer concentration may induce cellular stress at higher levels. A progressive decline in cell viability with increasing GA concentrations (from GC/GA1 to GC/GA3) was observed, implicating the cytotoxic potential of glutaraldehyde. This decrease is likely due to increased matrix rigidity and chemical reactivity, which could disrupt cellular functions[42,43]. In contrast, introducing HNTs (from GC/H1 to GC/H3) generally improved cell viability, with the highest HNT concentration showing viability comparable to the untreated control at lower dosages. This enhancement may be attributed to the HNTs' ability to modulate the matrix properties and, thus, reduce cytotoxicity. GC/GA2/H2 formulation maintained higher viability than high GA samples. It was comparable to high HNT samples, suggesting that a moderate level of cross-linking coupled with HNT reinforcement could synergistically improve the biocompatibility of the PECs[44,45]. These findings highlight the critical need to balance the components within biopolymeric drug delivery systems to optimise biocompatibility and therapeutic efficacy.

## Conclusion

In this study, we have developed a novel gelatin-halloysite nanotube-carrageenan polyelectrolyte complex for the controlled oral delivery of lipoic acid. The objective was to address the drug's poor water solubility and rapid degradation in acidic environments, significantly limiting its oral bioavailability and therapeutic efficacy.

The research successfully utilised the unique physicochemical properties of halloysite nanotubes (HNTs) and carrageenan to formulate a composite system that enhanced the encapsulation efficiency and provided controlled, *p*H-responsive drug release. *p*H-responsive release behaviour was a key focus of the study. *In vitro* release studies revealed that at *p*H 1.2 (simulating stomach conditions), the release of lipoic acid was minimal, effectively protecting the drug from the harsh gastric environment. Conversely, at *p*H 7.4 (intestinal conditions), there was a significant increase in drug release, demonstrating the system's effective response to environmental *p*H changes. Specifically, the release rate of lipoic acid at *p*H 7.4 was substantially higher, indicating successful targeting of the intestinal tract where absorption is optimised.

FTIR analysis confirmed the presence of key functional groups and their interactions, indicating effective encapsulation of lipoic acid within the matrix. XRD results showed a decrease in crystallinity in the drug-loaded samples, suggesting the amorphous dispersion of lipoic acid, which is favourable for enhancing its dissolution and bioavailability.

The composite's bioactivity was evaluated using glucose uptake and cell viability assays. The 2-NBDG glucose uptake assay demonstrated that the composite could enhance glucose uptake in L6 myotubes, indicative of the potential metabolic efficacy of the delivered lipoic acid. Moreover, the MTT assay for cell viability confirmed that the composite was non-toxic at various concentrations, further underscoring its suitability for biological applications.

This system's capacity to efficiently encapsulate and selectively release therapeutic agents in response to specific environmental triggers presents a valuable advancement in drug delivery. Future studies, particularly *in vivo*, will be crucial to fully validate the clinical applicability of this innovative drug delivery system.

## Acknowledgement

The authors would like to thank the Department of Chemical Sciences and SAIC, Tezpur University, for providing the facilities for this work. They are also grateful to Dr Suman Dasgupta, Assistant Professor, Department of Molecular Biology and Biotechnology, Tezpur University, and Ms Archana Sinha, Research Scholar, Department of Molecular Biology and Biotechnology, Tezpur University, for their help with the bioactivity assays.

## Conflict of Interest

There are no conflicts of interest.

## References

1 Shay K P, Moreau R F, Smith E J, Smith A R & Hagen T M, *Biochimica Biophysica Acta (BBA) - General Subjects*, 1790 (2009) 1149.
2 Smith A R & Hagen T M, *Biochem Soc Trans*, 31 (2003) 1447.
3 Salehi B, Berkay Yılmaz Y, Antika G, Boyunegmez Tumer T, Fawzi Mahomoodally M, Lobine D, Akram M, Riaz M, Capanoglu E, Sharopov F, Martins N, Cho W C & Sharifi-Rad J, *Biomolecules*, 9 (2019) 356.
4 Hua S, *Front Pharmacol*, 5 (2014), https://doi.org/10.3389/fphar.2014.00138.

5 Cózar-Bernal M J, Gallardo V, Sáez-Fernández E, Holgado M Á, Álvarez-Fuentes J, Fernández-Arévalo M & Arias J L, *Int J Pharm*, , 393 (2010) 162.

6 Dash M, Chiellini F, Ottenbrite R M & Chiellini E, *Prog Polym Sci*, 36 (2011) 981.

7 Young S, Wong M, Tabata Y & Mikos A G, *J Cont Rel*, 109 (2005) 256.

8 Lou L & Chen H, *Food Additives & Contaminants: Part A*, 40 (2023) 928.

9 Yang X, Yang Y, Yu H & Zhou Y, *Polymers (Basel)*, 15 (2023) 3538.

10 Sharma B, Malik P & Jain P, *Mater Today Comm,* , 16 (2018) 353.

11 Fakhruddin K, Hassan R, Khan M U A, Allisha S N, Razak S I A, Zreaqat M H, Latip H F M, Jamaludin M N & Hassan A, *Arabian J Chem*, 14 (2021) 103294.

12 Devi N & Maji T K, *Poly Bull*, 65 (2010) 347.

13 Al-Zebari N, Best S M & Cameron R E, *J Phys: Mat*, 2 (2018) 015003.

14 Sonawane R O & Patil S D, *Int J Poly Mat Poly Biomat*, 66 (2017) 812.

15 Gogoi P, Das M K, Ramteke A & Maji T K, *Int J Poly Mat Poly Biomat*, , 67 (2018) 543.

16 Devi N & Maji T K, *AAPS Pharm Sci Tech*, 10 (2009) 1412.

17 Banik N, Hussain A, Ramteke A, Sharma H K & Maji T K, *RSC Adv*, , 2 (2012) 10519.

18 Cassano R, Trombino S, Ferrarelli T, Mauro M V, Giraldi C, Manconi M, Fadda A M & Picci N, *J Biomed Mater Res A*, *100A* (2012) 536.

19 Tan J M, Karthivashan G, Arulselvan P, Fakurazi S & Hussein M Z, *J Nanomater*, 2014 (2014) https://doi.org/10.1155/2014/439873.

20 Pal D, Dasgupta S, Kundu R, Maitra S, Das G, Mukhopadhyay S, Ray S, Majumdar S S & Bhattacharya S, *Nat Med*, 18 (2012) 1279.

21 Khatun B, Rohilla S, Rather M A, Sinha A, Dasgupta S, Mandal M & Maji T K, *J Chem Sci*, 135 (2023) 16.

22 Mazumder S, Sinha A, Ghosh S, Sharma G C, Prusty B M, Manna D, Pal D, Pal C & Dasgupta S, *Pathog Dis*, 81 (2023) https://doi.org/10.1093/femspd/ftad019.

23 Kumar P, Nagarajan A & Uchil P D, *Cold Spring Harb Protoc*, 2018 (2018), pdb.prot095505 https://doi.org/10.1101/pdb.prot095505.

24 Fizir M, Dramou P, Dahiru N S, Ruya W, Huang T & He H, *Microchim Acta*, 185 (2018) 389 https://doi.org/10.1007/s00604-018-2908-1.

25 Dzeikala O, Prochon M & Sedzikowska N, *Int J Mol Sci*, 25 (2024) 4333.

26 Idumah C I, Hassan A, Ogbu J, Ndem J U & Nwuzor I C, *Compos Interfaces*, 26 (2019) 751.

27 Tipa C, Cidade M T, Borges J P, Costa L C, Silva J C & Soares P I P, *Nanomaterials*, 12 (2022) 3308.

28 Tokarev I & Minko S, *Adv Mat*, 22 (2010) 3446.

29 Das M P, R S P, Prasad K & Jv V, *Int J Pharm Pharm Sci*, 9 (2017) 239.

30 Campo V L, Kawano D F & Silva D B D, *Carbohy Polym*, 77 (2009) 167.

31 Bigi A, Cojazzi G, Panzavolta S, Rubini K & Roveri N, *Biomaterials*, 22 (2001) 763.

32 Atyaksheva L F & Kasyanov I A, *Petro Chem*, 61 (2021) 932.

33 Arnold R, Azzam W, Terfort A & Wöll C, *Langmuir*, 18 (2002) 3980.

34 Maeda H, Onodera T & Nakayama H, *J Incl Phenom Macrocycl Chem*, 68 (2010) 201.

35 Yallapu M M, Gupta B K, Jaggi M & Chauhan S C, *J Colloid Interface Sci*, 351 (2010) 19.

36 Biddeci G, Cavallaro G, Di Blasi F, Lazzara G, Massaro M, Milioto S, Parisi F, Riela S & Spinelli G, *Carbohydr Poly*, 152 (2016) 548.

37 Jawadi Z, Yang C, Haidar Z S, Santa Maria P L & Massa S, *Polymers (Basel)*, 14 (2022) 5459.

38 Yang M, Wei D, Mo C, Zhang J, Wang X, Han X, Wang Z & Xiao H, *Lipids Health Dis*, 12 (2013) 104.

39 Listenberger L L, Han X, Lewis S E, Cases S, Farese R V, Ory D S & Schaffer J E, *Proceed Nat Acad Sci*, 100 (2003) 3077.

40 Mikušová V & Mikuš P, *Int J Mol Sci*, 22 (2021) 9652.

41 Nelson K M, Dahlin J L, Bisson J, Graham J, Pauli G F & Walters M A, *J Med Chem*, 60 (2017) 1620.

42 George A & Shrivastav P S, *J Bioact Comp Poly*, 38 (2023) 368.

43 Oliveira A C S, Ugucioni J C & Borges S V, *J Food Proc Pres*, 45 (2021) (https://doi.org/10.1111/jfpp.15060).

44 Naumenko E A, Guryanov I D, Yendluri R, Lvov Y M & Fakhrullin R F, *Nanoscale*, 8 (2016) 7257.

45 Naumenko E & Fakhrullin R, *Biotechnol J*, 14 (2019) (https://doi.org/10.1002/biot.201900055).